

See discussions, stats, and author profiles for this publication at:  
<https://www.researchgate.net/publication/229628937>

# Stopped-flow studies of the mechanisms of ozone–alkene reactions in the gas phase propene and isobutene

ARTICLE *in* INTERNATIONAL JOURNAL OF CHEMICAL KINETICS · OCTOBER 1978

Impact Factor: 1.52 · DOI: 10.1002/kin.550101003

---

CITATIONS

27

---

READS

44

## 2 AUTHORS, INCLUDING:



[Robert Huie](#)

National Institute of Stand...

192 PUBLICATIONS 7,801

CITATIONS

SEE PROFILE

# Stopped-Flow Studies of the Mechanisms of Ozone-Alkene Reactions in the Gas Phase

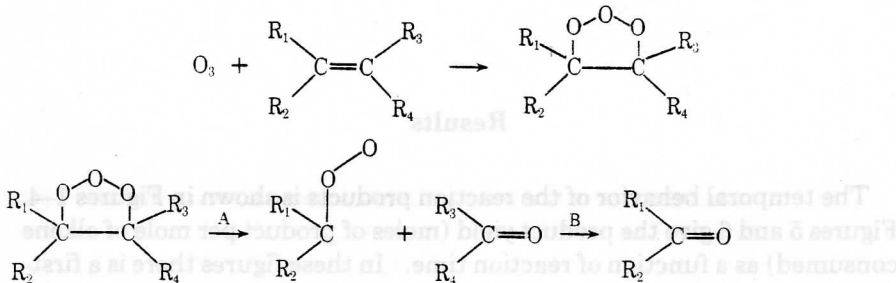
## Propene and Isobutene

JOHN T. HERRON and ROBERT E. HUIE

*Institute for Materials Research, National Bureau of Standards, Washington, DC 20234*

### Abstract

The reactions of ozone with propene and isobutene have been studied in the gas phase at 298°K and 530 Pa (4 torr) using a stopped-flow reactor coupled to a photoionization mass spectrometer. Reactant and product concentrations were followed as a function of reaction time. The major reaction products monitored were CH<sub>2</sub>O, CH<sub>3</sub>CHO, CO<sub>2</sub>, and H<sub>2</sub>O from the propene reaction, and CH<sub>2</sub>O, (CH<sub>3</sub>)<sub>2</sub>CO, CO<sub>2</sub>, and H<sub>2</sub>O from the isobutene reaction. The observations were interpreted on the basis of the Criegee mechanism for ozonolysis in solution:



for which we find  $k_A \approx k_B$ . In the gas phase the carbene peroxy radical is postulated to isomerize and decompose into molecular and free-radical products.

### Introduction

In the previous paper in this series [1] we reported the results of a study of the reaction of ozone with ethylene. Through the use of computer modeling, a detailed reaction mechanism was derived. We report here similar data for the propene and isobutene (2-methylpropene) reactions. Due to the greater complexity and uncertainty of the secondary reactions, we have not been able to derive a definitive mechanism. Modeling studies,

however, have helped to clarify some of the general features of the reactions, and point out those areas in which additional work is needed.

## Experimental

The experimental method has been discussed in detail previously [1]. Briefly, the apparatus consists of a 300-cm<sup>3</sup> reactor coupled to a beam sampling mass spectrometer using rare-gas resonance lamps as photoionization sources. A mixture of about 5% ozone in oxygen was premixed with olefin and flowed through the reactor at a total pressure of 530 Pa (4 torr) and a temperature of 298°K. The reactor could be isolated by means of solenoid valves and the partial pressures of reactants and products monitored with the mass spectrometer. Calibrations were carried out using gas mixtures at the same total pressure as used in the experiments. No calibration was made for formic acid or for the peak labeled *m/e* (mass to charge ratio) of 74 in Figure 2. In both cases the sensitivity was arbitrarily taken to be that of acetic acid.

## Results

The temporal behavior of the reaction products is shown in Figures 1-4. Figures 5 and 6 give the product yield (moles of product per mole of alkene consumed) as a function of reaction time. In these figures there is a first-order decay component ( $k \approx 2.5 \times 10^{-3} \text{ sec}^{-1}$ ) due to pumping out of the contents of the reactor through the sampling orifice. The product yields for  $t = 0$ , extrapolated from Figures 5 and 6, are listed in Table I along with the results for the ethylene reaction. These  $t = 0$  yields are not necessarily the same as the stoichiometry of the initial reaction since some secondary reactions, particularly those involving H, OH, and HO<sub>2</sub>, are so fast that they are essentially instantaneous on our time scale.

As in the ethylene study, CO and H<sub>2</sub>, which are expected to be major products, were not measured. Some minor product peaks were found but not identified or studied in detail. An example is the product listed as *m/e* = 74 in the propene reaction (Figs. 2 and 5). A peak at *m/e* = 32 was found for both propene and isobutene which could be methanol or O<sub>2</sub> (1Δ<sub>g</sub>). However, severe interference from photoelectron ionization of the very large oxygen background made a positive identification impossible.

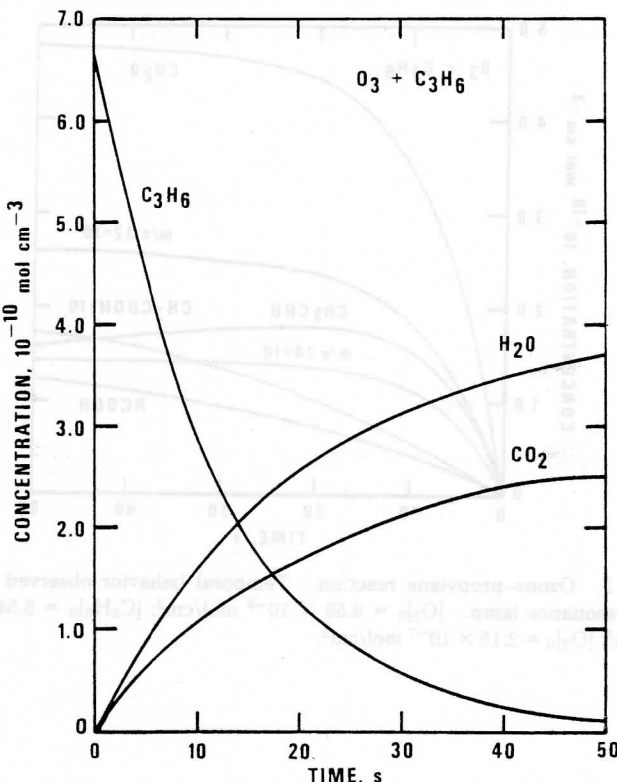


Figure 1. Ozone-propylene reaction. Temporal behavior observed using a helium resonance lamp.  $[O_3]_0 = 9.91 \times 10^{-9} \text{ mol/cm}^3$ ;  $[C_3H_6]_0 = 6.61 \times 10^{-10} \text{ mol/cm}^3$ ;  $[O_2]_0 = 2.15 \times 10^{-7} \text{ mol/cm}^3$ .

### Discussion

#### General Observations

In our study of the ozone-ethylene reaction [1], it was established that secondary free-radical reactions play a very important role in the overall chemistry. This was apparent from the observation that the product yields were not constant; the yield of products which might be expected to be reactive toward free radicals decreased with time, and the yield of products which might also be products of radical reactions, such as  $H_2O$ , increased. This same behavior has now been observed in the propene and isobutene reactions (see Figs. 5 and 6). In the propene system, formaldehyde and acetaldehyde are consumed in secondary reactions while carbon dioxide, water, and the organic acids are produced. For isobutene, formaldehyde

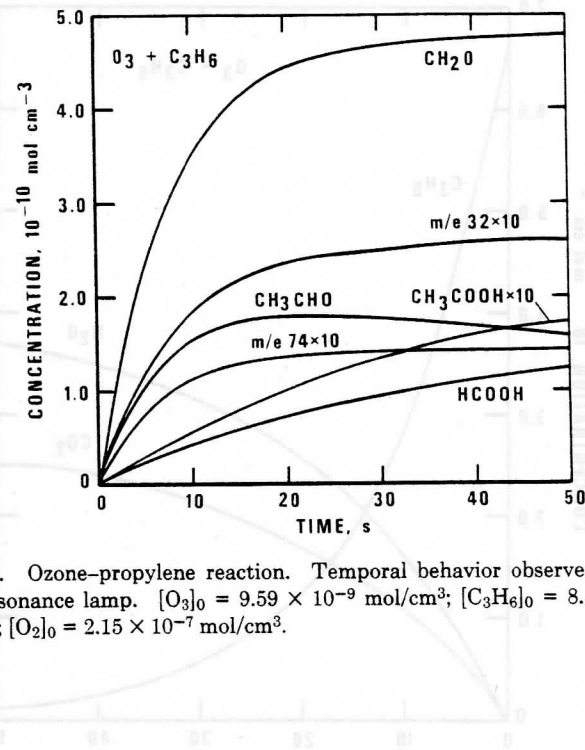


Figure 2. Ozone-propylene reaction. Temporal behavior observed using an argon resonance lamp.  $[O_3]_0 = 9.59 \times 10^{-9} \text{ mol/cm}^3$ ;  $[C_3H_6]_0 = 8.54 \times 10^{-10} \text{ mol/cm}^3$ ;  $[O_2]_0 = 2.15 \times 10^{-7} \text{ mol/cm}^3$ .

is also consumed, and carbon dioxide, water, and the organic acids are produced. Acetone, however, is unaffected by secondary reactions.

There is evidence from other studies that, at low pressures, free radicals are formed in ozone-alkene systems [2-4]. In particular, the observation of the OH Meinel bands [3], which are known to arise from the reaction  $H + O_3 \rightarrow OH^\cdot + O_2$ , is strong evidence that hydrogen atoms are generated. In addition, the observation that the rate of decay of ozone in the presence of excess alkene is slowed by the addition of molecular oxygen suggests the presence of free radicals which can be scavenged by oxygen [3-8] (Note, however, that under our experimental conditions, hydrogen atoms are not scavenged by oxygen). These free radicals initiate a large number of secondary reactions, many of which are very fast relative to the ozone-alkene reaction.

To obtain information on the nature of the elementary ozone-alkene reactions, modeling studies were carried out. We used the computer modeling program of Brown [9] based on the Gear method [10] for handling "stiff" systems, and the elementary reactions listed in Tables II and III for propene and isobutene, respectively. We start with the assumption that ozone adds across the double bond forming the primary ozonide, which falls

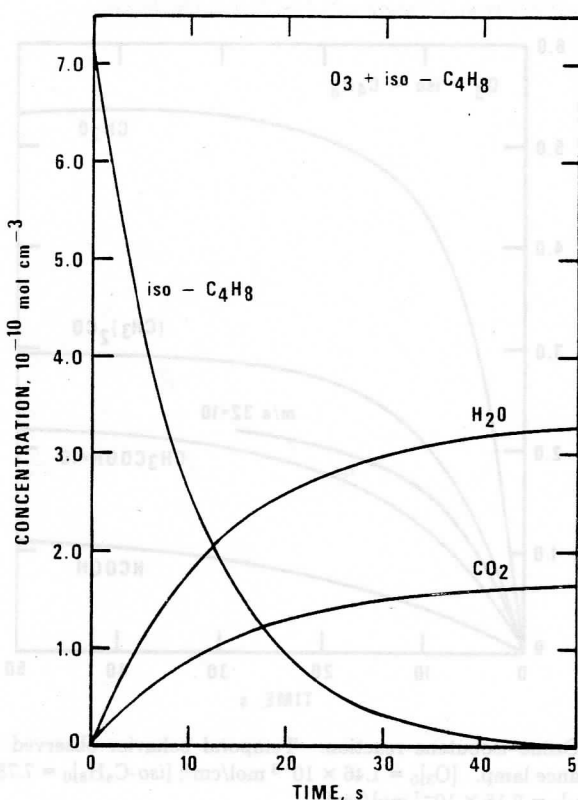
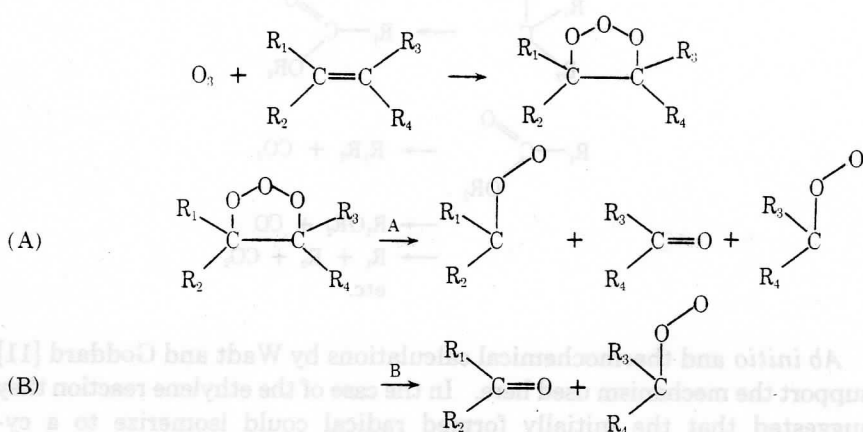


Figure 3. Ozone-isobutene reaction. Temporal behavior observed using a helium resonance lamp.  $[O_3]_0 = 1.08 \times 10^{-8} \text{ mol/cm}^3$ ;  $[iso-C_4H_8]_0 = 7.18 \times 10^{-10} \text{ mol/cm}^3$ ;  $[O_2]_0 = 2.15 \times 10^{-7} \text{ mol/cm}^3$ .

apart, as in the Criegee mechanism, to an aldehyde or ketone and a carbene peroxy radical:



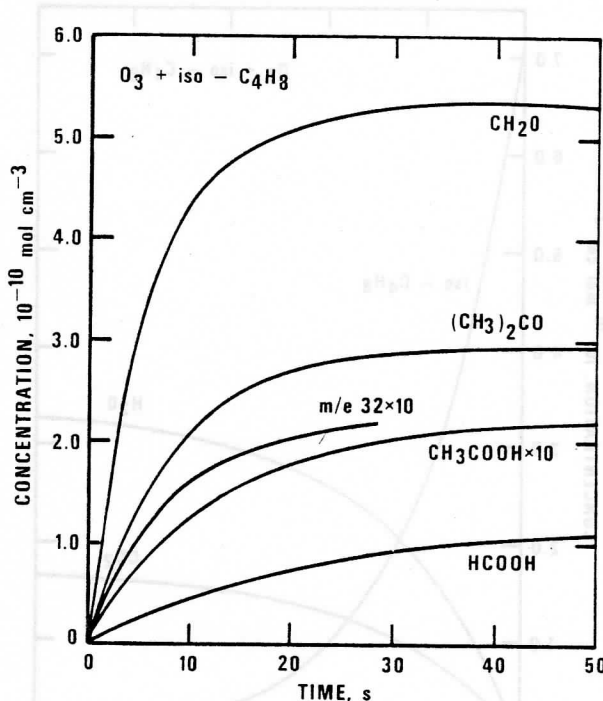
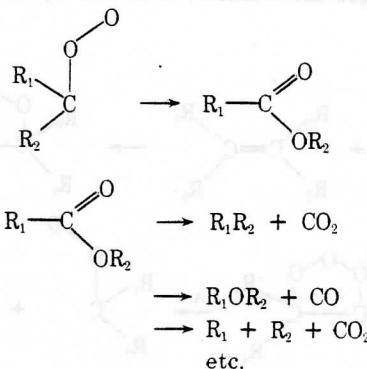


Figure 4. Ozone-isobutene reaction. Temporal behavior observed using an argon resonance lamp.  $[O_3]_0 = 1.46 \times 10^{-8} \text{ mol/cm}^3$ ;  $[iso-C_4H_8]_0 = 7.78 \times 10^{-10} \text{ mol/cm}^3$ ;  $[O_2]_0 = 2.15 \times 10^{-7} \text{ mol/cm}^3$ .

We then assume that the radical rearranges to a hot acid or ester which may then decompose to molecular or free-radical products, for example,



*Ab initio* and thermochemical calculations by Wadt and Goddard [11] support the mechanism used here. In the case of the ethylene reaction they suggested that the initially formed radical could isomerize to a cy-

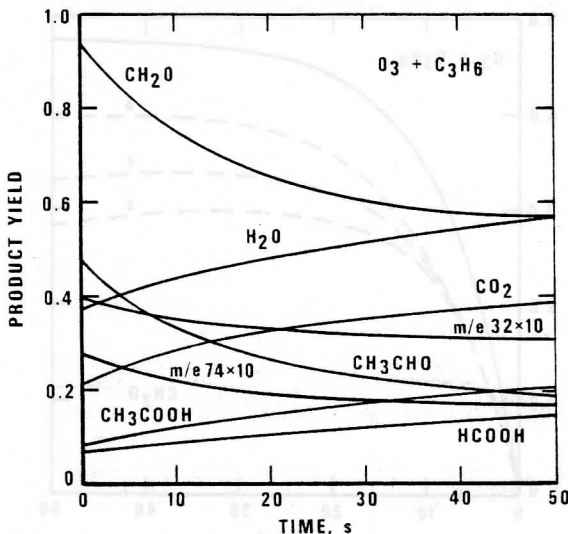


Figure 5. Ozone-propylene reaction. Product yield ( $\Delta$  product/ $\Delta$  propylene). Based on data from Figures 1 and 2. Note that no correction for pump-out has been made.

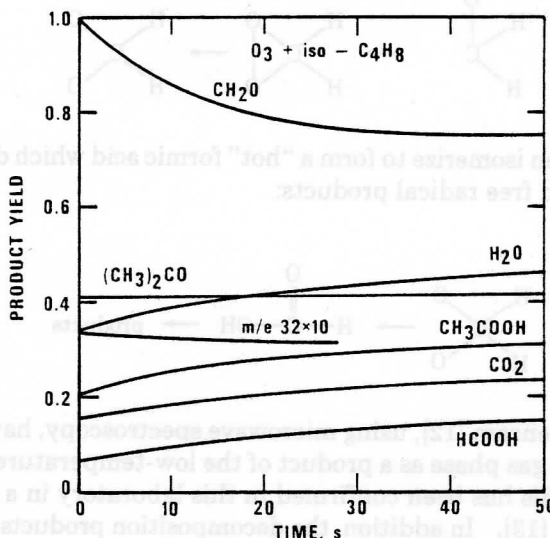


Figure 6. Ozone-isobutene reaction. Product yield ( $\Delta$  product/ $\Delta$  isobutene). Based on data from Figures 3 and 4. Note that no correction for pump-out has been made.

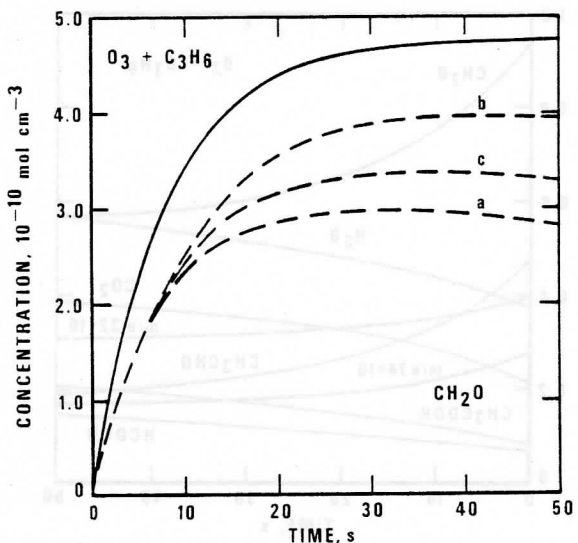
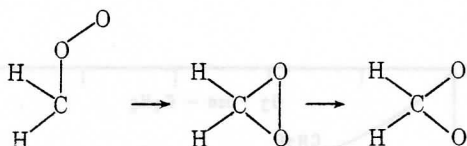
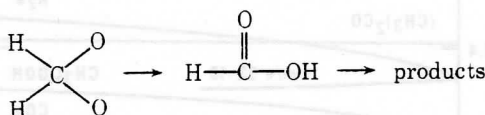


Figure 7. Comparison of observed (—) and calculated (---) formaldehyde profiles in the ozone-propylene reaction. Curve a— $(k_{3a} + k_{4a})/(k_3 + k_4) = 1$ ; curve b— $k_{4b}/(k_3 + k_4) = 1$ ; curve c— $(k_{3a} + k_{4a})/(k_3 + k_4) = k_{4b}/(k_3 + k_4) = 0.5$ .

clic peroxide (dioxirane) which would open to a dioxyl radical:



This could then isomerize to form a "hot" formic acid which decomposes to molecular and free radical products:



Lovas and Suenram [12], using microwave spectroscopy, have detected dioxirane in the gas phase as a product of the low-temperature ozonolysis of ethylene. This has been confirmed in this laboratory in a mass-spectrometric study [13]. In addition, the decomposition products  $\text{H}_2$  and  $\text{CO}$  were observed.

For the terminal alkenes, propene and isobutene, one of the decomposition modes of the initial adduct leads to the methylene peroxy radical

TABLE I. Product yield ( $\Delta$  product/ $\Delta$  olefin) at  $t = 0$ .

	$C_2H_4^a$	$C_3H_6$	$iso-C_4H_8$
$CH_2O$	1.0	0.94	1.0
$CH_3CHO$	-	0.45	-
$(CH_3)_2CO$	-	-	0.41
HCOOH	0.06	0.04	0.06
$CH_3COOH$	-	0.01	0.02
m/e 32	0.03 <sup>b</sup>	0.04 <sup>c</sup>	0.03 <sup>c</sup>
$CO_2$	0.27	0.24	0.16
$H_2O$	0.67	0.38	0.35
CO	(0.67) <sup>d</sup>	(0.6) <sup>e</sup>	
$H_2$	(0.27) <sup>d</sup>		
Carbon balance <sup>f</sup>	68(102)	73(93)	63
Hydrogen balance <sup>f</sup>	90(103)		69

<sup>a</sup> From [1].<sup>b</sup> Mass 36 using  $C_2D_4$  reactant.<sup>c</sup> May contain contribution from  $O_2^{1\Delta_g}$ .<sup>d</sup> Estimate based on mechanism.<sup>e</sup> Estimate based on [4]. This is probably high, corresponding to  $t > 0$ .<sup>f</sup> Figures in parentheses include estimated contribution from CO and  $H_2$ .

$CH_2OO$ , the same intermediate as is formed in the reaction of ozone and ethylene. In our earlier paper [1] we were able to determine the decomposition routes for  $CH_2OO$ , and we have incorporated this information into Tables II and III. What we need to know now is the ratio  $k_A/k_B$  and the branching ratios for the decomposition of  $CH_3CHOO$  and  $(CH_3)_2COO$ .

### Propene

The reaction of ozone with propene leads to the radicals  $CH_2OO$  and  $CH_3CHOO$  [reactions (1a) and (1b)]. The ratio of these two paths is not known, but the yield of  $CH_3CHO$  at zero time, 0.45, suggests  $k_{1a}/k_{1b} = 1.22$ . This value was used in the initial modeling calculations. As noted above, we have adopted the formalism of having  $CH_3CHOO$  rearrange to a hot acid or ester which may then decompose [reactions (3a)–(3e) and (4a)–(4d)]. Note that some of the reactions are equivalent and that reactions having more than two products represent the sum of a pair of consecutive reactions, that is, reaction (3a) is more properly written as  $CH_3CHOO \rightarrow [CH_3COOH]^+ \rightarrow CH_3 + HCO_2$  followed by  $HCO_2 \rightarrow H + CO_2$ .

Experimentally, we have found that  $CH_2CO$  and the organic acids and esters are at best minor products. Gas chromatographic analysis indicated that  $CH_4$  was also a minor product. Therefore we ignore reactions (3c)–(3e), (4c), and (4d), leaving three distinguishable reaction channels: (3a)

TABLE II. Mechanism of the ozone-propylene reaction at low pressure.

Reaction	Rate Constant $\text{cm}^3 \text{mol}^{-1} \text{s}^{-1}$	Ref.
1a $\text{C}_3\text{H}_6 + \text{O}_3 \rightarrow \text{CH}_2\text{O} + \text{CH}_3\text{CHO}$	$3.2 \times 10^6$	6 <sup>a</sup>
1b $\quad \quad \quad + \text{CH}_2\text{OO} + \text{CH}_3\text{CHO}$	$3.2 \times 10^6$	
2a $\text{CH}_2\text{OO} + [\text{HCOOH}]^+ \rightarrow \text{CO} + \text{H}_2\text{O}$	67%	1
2b $\quad \quad \quad \rightarrow \text{CO}_2 + \text{H}_2$	18%	
2c $\quad \quad \quad \rightarrow \text{CO}_2 + 2\text{H}$	9%	
2d $\quad \quad \quad \rightarrow \text{HCOOH} ?$	6%	
3a $\text{CH}_3\text{CHO} \rightarrow [\text{CH}_3\text{COOH}]^+ \rightarrow \text{CH}_3 + \text{H} + \text{CO}_2$		
3b $\quad \quad \quad \rightarrow \text{CH}_3 + \text{CO} + \text{OH}$		
3c $\quad \quad \quad \rightarrow \text{CH}_4 + \text{CO}_2$		
3d $\quad \quad \quad \rightarrow \text{CH}_2\text{CO} + \text{H}_2\text{O}$		
3e $\quad \quad \quad \rightarrow \text{CH}_3\text{COOH} ?$		
4a $\text{CH}_3\text{CHO} + [\text{HCOOCH}_3]^+ \rightarrow \text{CH}_3 + \text{H} + \text{CO}_2$		
4b $\quad \quad \quad \rightarrow \text{CH}_3\text{O} + \text{HCO}$		
4c $\quad \quad \quad \rightarrow \text{CH}_4 + \text{CO}_2$		
4d $\quad \quad \quad \rightarrow \text{HCOOCH}_3 ?$		
5 $\text{H} + \text{C}_3\text{H}_6 \rightarrow \text{C}_3\text{H}_7(\text{R})$	$2.5 \times 10^{12}$	31
6 $\text{H} + \text{O}_3 \rightarrow \text{OH} + \text{O}_2$	$1.6 \times 10^{13}$	30
7 $\text{OH} + \text{C}_3\text{H}_6 \rightarrow \text{C}_3\text{H}_6\text{OH} (\text{R})$	$9.0 \times 10^{12}$	30
8 $\text{OH} + \text{O}_3 \rightarrow \text{HO}_2 + \text{O}_2$	$2.8 \times 10^{10}$	30
9 $\text{HO}_2 + \text{O}_3 \rightarrow \text{OH} + 2\text{O}_2$	$9.0 \times 10^8$	30
10 $\text{OH} + \text{CH}_2\text{O} \rightarrow \text{H}_2\text{O} + \text{HCO}$	$8.4 \times 10^{12}$	30
11 $\text{OH} + \text{CH}_3\text{CHO} \rightarrow \text{H}_2\text{O} + \text{CH}_3\text{CO}$	$8.4 \times 10^{12}$	b
12 $\text{HCO} + \text{O}_2 \rightarrow \text{HO}_2 + \text{CO}$	$3.4 \times 10^{12}$	30
13 $\text{CH}_3\text{O} + \text{O}_2 \rightarrow \text{CH}_2\text{O} + \text{HO}_2$	$2 \times 10^7$	16, 17, 32
14 $\text{CH}_3 + \text{O}_2 \rightarrow \text{CH}_3\text{O}_2$	$2 \times 10^{10}$	33
15 $\text{CH}_3 + \text{O}_3 \rightarrow \text{CH}_2\text{O} + \text{H} + \text{O}_2$	$5.5 \times 10^{11}$	14
16 $\text{CH}_3\text{CO} + \text{O}_2 \rightarrow \text{CH}_3 + \text{CO}_2$	$1 \times 10^{11}$ f	c
17 $\text{R} + \text{O}_2 + \text{RO}_2$	$1 \times 10^{11}$	c, g
18 $\text{R} + \text{O}_3 \rightarrow \text{RO}^+ + \text{O}_2$	$5.5 \times 10^{11}$	c
19 $2\text{HO}_2 \rightarrow \text{H}_2\text{O}_2 + \text{O}_2$	$3.4 \times 10^{12}$	30
20 $\text{HO}_2 + \text{OH} \rightarrow \text{H}_2\text{O} + \text{O}_2$	$1 \times 10^{13}$	d
21 $\text{HO}_2 + \text{CH}_3\text{O} \rightarrow \text{CH}_3\text{OH} + \text{O}_2$	$1 \times 10^{12}$	23 <sup>e</sup>
22 $\text{HO}_2 + \text{CH}_3\text{O}_2 \rightarrow \text{CH}_3\text{OOH} + \text{O}_2$	$4 \times 10^{10}$	23 <sup>e</sup>
23 $\text{HO}_2 + \text{RO}_2 \rightarrow \text{ROOH} + \text{O}_2$	$1 \times 10^{11}$	c
24 $2\text{CH}_3\text{O} + \text{CH}_2\text{O} + \text{CH}_3\text{OH} \rightarrow$	$1.5 \times 10^{13}$	23
25 $\text{CH}_3\text{O} + \text{OH} \rightarrow \text{CH}_2\text{O} + \text{H}_2\text{O}$	$3 \times 10^{13}$	23 <sup>e</sup>
26 $\text{CH}_3\text{O} + \text{CH}_3\text{O}_2 \rightarrow \text{CH}_2\text{O} + \text{CH}_3\text{OOH}$	$2 \times 10^{12}$	23 <sup>e</sup>
27 $\text{CH}_3\text{O} + \text{RO}_2 \rightarrow$	$1 \times 10^{11}$	c
28a $2\text{CH}_3\text{O}_2 \rightarrow 2\text{CH}_3\text{O} + \text{O}_2$	$7 \times 10^{10}$	d
28b $\quad \quad \quad \rightarrow \text{CH}_2\text{O} + \text{CH}_3\text{OH} + \text{O}_2$	$7 \times 10^{10}$	d
29 $\text{CH}_3\text{O}_2 + \text{OH} \rightarrow \text{CH}_3\text{OH} + \text{O}_2$	$1 \times 10^{12}$	c
30 $\text{RO}_2 + \text{RO}_2 \rightarrow$	$1 \times 10^{11}$	c
31 $\text{RO}_2 + \text{OH} \rightarrow \text{ROH} + \text{O}_2$	$1 \times 10^{12}$	c

<sup>a</sup> Based on the reported total rate constant of  $6.36 \times 10^6 \text{ cm}^3/\text{mol}\cdot\text{sec}$ .<sup>b</sup> The rate constant was taken to be the same as for reaction (10).<sup>c</sup> Estimated, this work.<sup>d</sup> Estimate based on range of reported values in [30].<sup>e</sup> Estimated.<sup>f</sup> The reaction is not elementary.<sup>g</sup> R includes all alkyl radicals other than  $\text{CH}_3$ .

or (4a), (3b), and (4b). The rest of the reactions in Table II [reactions (5) through (31)] were, when possible, assigned rate constants from the literature. Often, however, the rate constants and mechanisms are based on analogies or are just plain guesswork. This problem will be discussed in greater detail later.

There are no data available which would allow us to choose the branching ratios for the remaining decomposition channels. In order to assess the effect of various choices, the model was run using the possible extreme values (a)  $(k_{3a} + k_{4a})/(k_3 + k_4) = 1$ ; (b)  $k_{4b}/(k_3 + k_4) = 1$ ; and (c)  $(k_{3a} + k_{4a})/(k_3 + k_4) = k_{4b}/(k_3 + k_4) = 0.5$ . We did not carry out a run using  $k_{3b}/(k_3 + k_4) = 1$  since the rapid conversion of H to OH makes it almost identical to condition (a), except in the production of CO<sub>2</sub>, which would be identical to condition (b). The ratios used correspond not only to differing amounts of CO and CO<sub>2</sub> produced in the decomposition, but also to the chemical activity of the overall reaction, as reflected in the extent to which aldehydes are consumed in secondary reactions. For condition (a), one CH<sub>3</sub> and one H are produced in the decomposition. These, especially H, are more active radicals than the CH<sub>3</sub>O and CHO produced under condition (b). Condition (c) is intermediate in activity.

For all of these possibilities, it was apparent that the OH concentration was quite high, about  $10^{-15}$  mol/cm<sup>3</sup> after 5 sec. For the intermediate condition, then, about 20% of the propene is lost through secondary reac-

TABLE III. Mechanism of the ozone-isobutene reaction at low pressure.

Reaction	Rate Constant cm <sup>3</sup> mol <sup>-1</sup> s <sup>-1</sup>	Ref.
32a i-C <sub>4</sub> H <sub>8</sub> + O <sub>3</sub> → CH <sub>2</sub> O + (CH <sub>3</sub> ) <sub>2</sub> COO	$3.2 \times 10^6$	6 <sup>a</sup>
32b → CHOO + (CH <sub>3</sub> ) <sub>2</sub> CO	$3.8 \times 10^6$	
2a CH <sub>2</sub> OO + [HCOOH] <sup>+</sup> → CO + H <sub>2</sub> O	67%	1
2b → CO <sub>2</sub> + H <sub>2</sub>	18%	
2c → CO <sub>2</sub> + 2H	9%	
2d → HCOOH ?	6%	
33a (CH <sub>3</sub> ) <sub>2</sub> COO + [CH <sub>3</sub> COOCH <sub>3</sub> ] <sup>+</sup> → 2CH <sub>3</sub> + CO <sub>2</sub>		
33b → CH <sub>3</sub> O + CH <sub>3</sub> + CO		
33c → CH <sub>3</sub> O + CH <sub>3</sub> CO		
34 H + i-C <sub>4</sub> H <sub>8</sub> → C <sub>4</sub> H <sub>9</sub> (R)	$2.3 \times 10^{12}$	33
6 H + O <sub>3</sub> → OH + O <sub>2</sub>	$1.6 \times 10^{13}$	30
35 OH + i-C <sub>4</sub> H <sub>8</sub> → C <sub>4</sub> H <sub>9</sub> OH (R)	$9.0 \times 10^{12}$	b

FOLLOWED BY REACTIONS (8) THROUGH (31) FROM TABLE 2.

<sup>a</sup> Based on the reported total rate constant of  $7.01 \times 10^6$  cm<sup>3</sup>/mol·sec.

<sup>b</sup> The rate constant was taken to be the same as for reaction (7), Table II. Recent measurements indicate that the rate constant is about twice as great as the value used here [38,39].

tions with OH, even near  $t = 0$ . Therefore, 0.45 is probably not correct for the primary yield of  $\text{CH}_3\text{CHO}$ . We have increased the value to 0.5 for the subsequent modeling calculations.

The results of modeling runs using conditions (a), (b), and (c), with a value of  $k_{1a}/k_{1b} = 1$ , are shown in Figures 7–10, along with the observed product curves. Examination of these figures, although not leading to a definitive statement of the relative importance of the possible reaction channels, does allow us to reach the following conclusions:

(a) The intuitively simple decomposition mode (3a) [or (4a)] shown as curve a in the figures, leads to a much higher  $\text{CO}_2$  concentration than is observed. This indicates that other reactions such as (3b) or (4b) followed by oxidation of  $\text{HCO}$  lead to the formation of  $\text{CO}$  and consequently reduce the amount of  $\text{CO}_2$  which is formed. On the other hand, eliminating reactions (3a) and (4a), as illustrated in the curves labeled b in Figures 7–10, leads to a great underestimate of the  $\text{CO}_2$  concentration. Allowing both types of reaction to proceed at equal rates gives curves c, which (except for  $\text{CH}_2\text{O}$ ) fit the observed data quite well.

(b) Different primary decomposition modes lead to different degrees of chemical activity. Thus reactions such as (3a) or (4a) lead ultimately to OH radicals which in turn attack the aldehydes present in the system. As

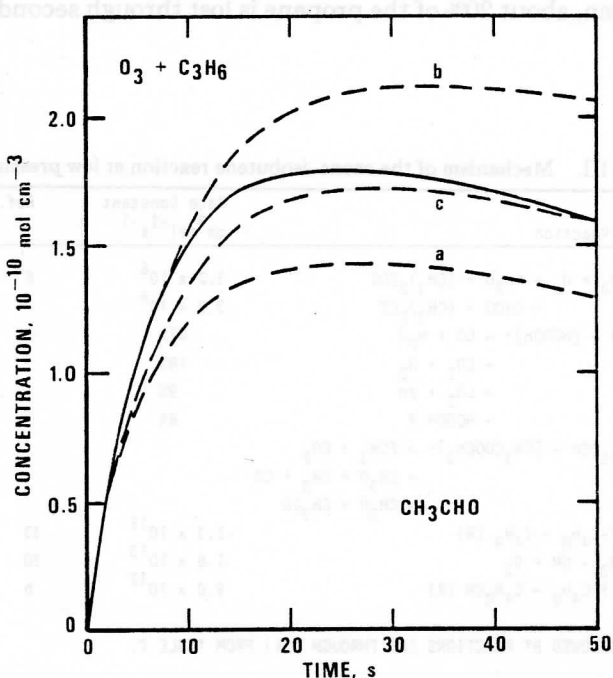


Figure 8. Comparison of observed (—) and calculated (---) acetaldehyde profiles in the ozone-propylene reaction. Calculated profiles correspond to rate constant ratios of Figure 7.

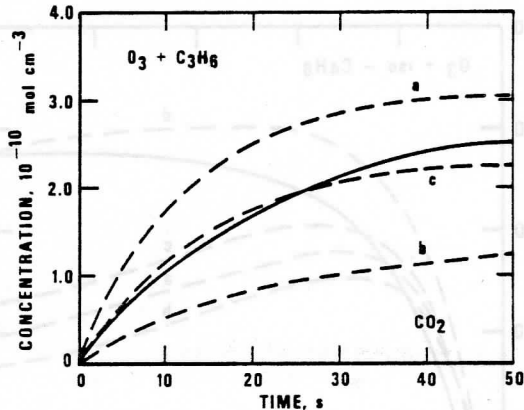


Figure 9. Comparison of observed (—) and calculated (---) carbon dioxide profiles in the ozone-propylene reaction. Calculated profiles correspond to rate constant ratios of Figure 7.

shown by curves a in the figures, this situation is one in which both  $\text{CH}_2\text{O}$  and  $\text{CH}_3\text{CHO}$  are consumed so rapidly by OH reactions that the concentrations lie below the observed values. If we go to a less chemically active reaction such as (4b), shown as curve b, then we find that  $\text{CH}_3\text{CHO}$  is consumed so much slower than before, that it actually comes out higher than observed. The concentration of  $\text{CH}_2\text{O}$ , on the other hand, still is less than observed. We interpret this to mean that there is an additional source term for  $\text{CH}_2\text{O}$  in this system, probably involving secondary reactions. A plausible source of additional  $\text{CH}_2\text{O}$  is via reaction (18). If  $\text{RO}^\ddagger$  decomposes to a methyl radical, additional  $\text{CH}_2\text{O}$  would be produced through reactions (14) and (15). Modeling, however, shows that this step could account for only a small portion of the observed discrepancy.

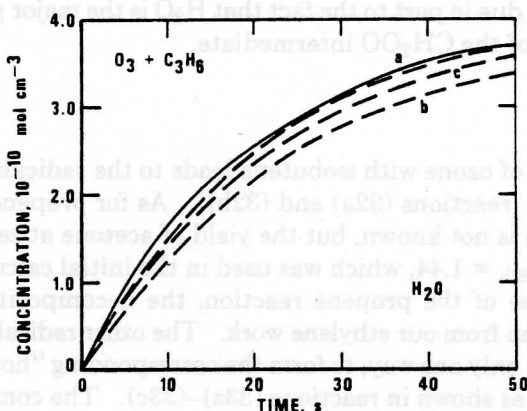


Figure 10. Comparison of observed (—) and calculated (---) water profiles in the ozone-propylene reaction. Calculated profiles correspond to rate constant ratios of Figure 7.

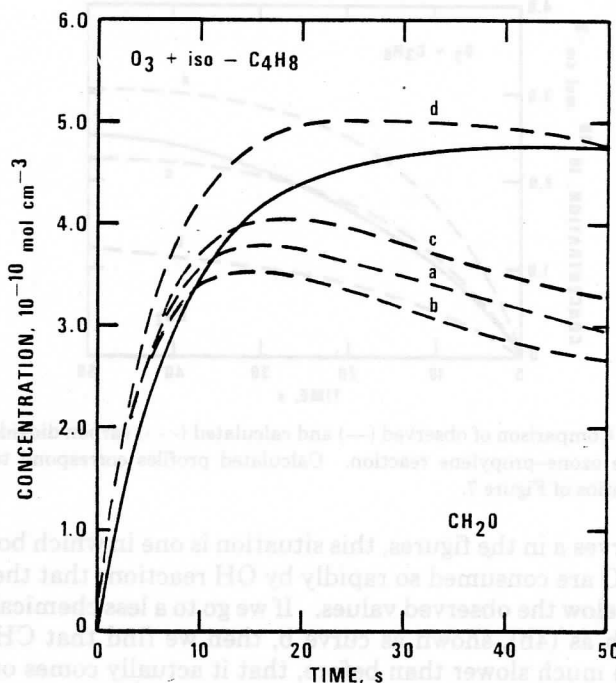


Figure 11. Comparison of observed (—) and calculated (---) formaldehyde profiles in the ozone-isobutene reaction. Curve a— $k_{34a}/k_{34} = k_{34b}/k_{34} = 0.5$ ; curve b— $k_{34a}/k_{34} = 1$ ; curve c— $k_{34b}/k_{34} = 1$ . For curve d, see text.

The best fit for the  $\text{CH}_3\text{CHO}$  observations also corresponds to curve c, which as before means that both types of reactions could proceed at roughly equal rates.

(c) The predicted  $\text{H}_2\text{O}$  profiles are insensitive to the particular model chosen. This is due in part to the fact that  $\text{H}_2\text{O}$  is the major product of the decomposition of the  $\text{CH}_2\text{OO}$  intermediate.

### Isobutene

The reaction of ozone with isobutene leads to the radicals  $\text{CH}_2\text{OO}$  and  $\text{CH}_3(\text{CH}_3)\text{COO}$  [reactions (32a) and (32b)]. As for propene, the ratio of these two paths is not known, but the yield of acetone at zero time, 0.41, suggests  $k_{32a}/k_{32b} = 1.44$ , which was used in the initial calculations.

As in the case of the propene reaction, the decomposition routes of  $\text{CH}_2\text{OO}$  are taken from our ethylene work. The other radical,  $(\text{CH}_3)_2\text{COO}$ , can isomerize in only one way, to form the corresponding "hot" ester which can decompose as shown in reactions (33a)–(33c). The complete mechanism is given in Table III.

In order to assess the relative importance of the three decomposition routes, their ratios were varied and the calculated concentration profiles

compared to the measured profiles. The ratios used were (a)  $k_{33a}/k_{33} = k_{33b}/k_{33} = 0.5$ ; (b)  $k_{33a}/k_{33} = 1$ ; and (c)  $k_{33b}/k_{33} = 1$ . An OH concentration of  $\sim 5 \times 10^{-15}$  mol/cm<sup>3</sup> was calculated after 5 sec, suggesting that about one third of the isobutene is lost due to reaction with OH. Therefore the primary yield of acetone must be greater than 0.41. We chose 0.54 since this value led to the best fit of the acetone data. The calculated and observed profiles, using  $k_{32a}/k_{32b} = 0.85$  are compared in Figures 11-14.

From an examination of these figures, we draw the following conclusions:

(a) The simple decomposition mode, reaction (33a), shown as curve b in the figures, greatly overestimates the CO<sub>2</sub> yield. To reduce the amount of CO<sub>2</sub> produced, we look for alternative reaction routes which lead to CO rather than CO<sub>2</sub>. One possibility is reaction (33b). Reaction (33c) in which the CH<sub>3</sub>CO would be further oxidized to yield CO appears to be unlikely (see further). If we choose  $k_{33b}/k_{33} = 1$ , however, the CO<sub>2</sub> concentration profile shown as curve c is much too low. A much better fit is obtained by setting  $k_{33a}/k_{33} = k_{33b}/k_{33} = 0.5$ , as shown in curve a.

(b) Reaction (33a) leads to a more chemically active system than does reaction (33b) because of the ultimate production of OH from secondary reaction initiated by CH<sub>3</sub>. This in turn reduces the CH<sub>2</sub>O profile because

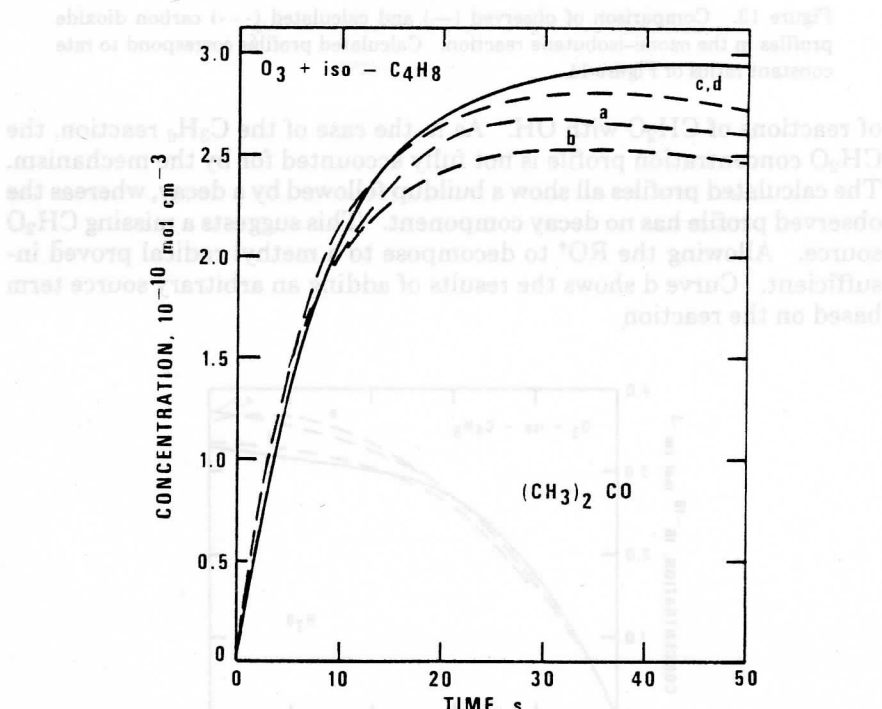


Figure 12. Comparison of observed (—) and calculated (---) acetone profiles in the ozone-isobutene reaction. Calculated profiles correspond to rate constant ratios of Figure 11.

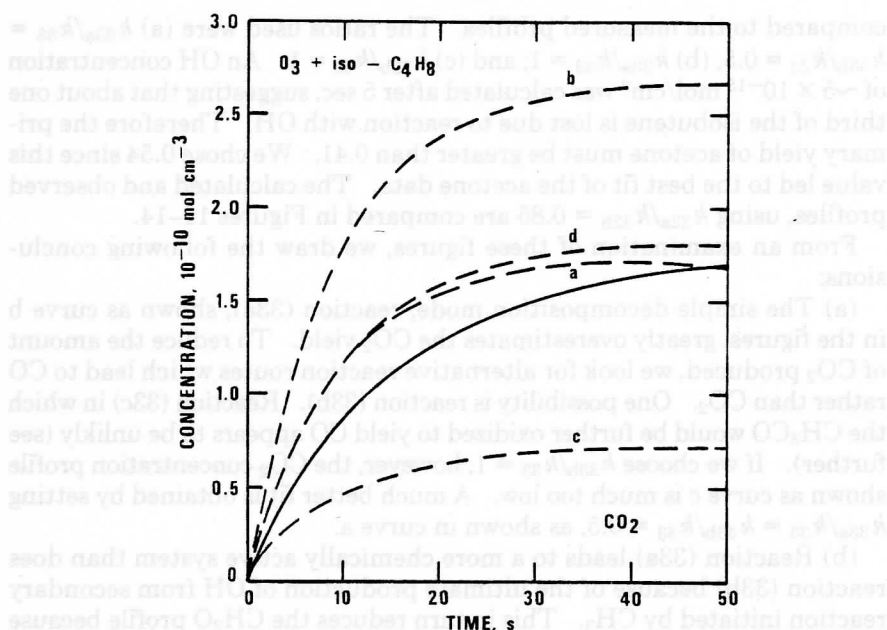


Figure 13. Comparison of observed (—) and calculated (---) carbon dioxide profiles in the ozone-isobutene reaction. Calculated profiles correspond to rate constant ratios of Figure 11.

of reactions of CH<sub>2</sub>O with OH. As in the case of the C<sub>3</sub>H<sub>6</sub> reaction, the CH<sub>2</sub>O concentration profile is not fully accounted for by the mechanism. The calculated profiles all show a buildup followed by a decay, whereas the observed profile has no decay component. This suggests a missing CH<sub>2</sub>O source. Allowing the RO<sup>†</sup> to decompose to a methyl radical proved insufficient. Curve d shows the results of adding an arbitrary source term based on the reaction

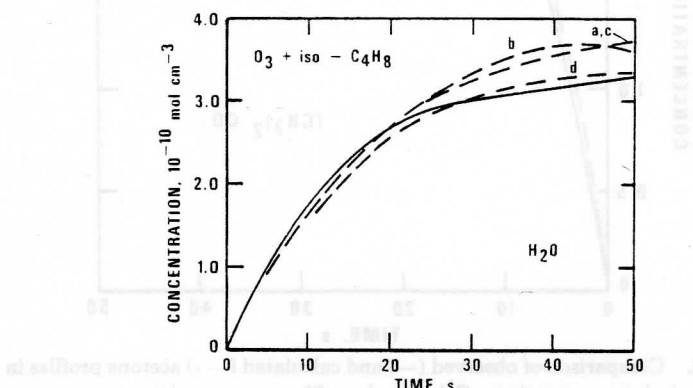
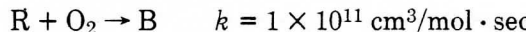
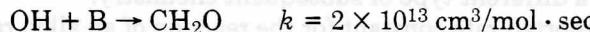


Figure 14. Comparison of observed (—) and calculated (---) water profiles in the ozone-isobutene reaction. Calculated profiles correspond to rate constant ratios of Figure 11.



where R includes the  $C_4H_9$  and  $C_4H_8OH$  radicals, followed by



We have not made any attempt to fit the data exactly using this pair of reactions. The object is simply to illustrate one possible type of  $CH_2O$  source.

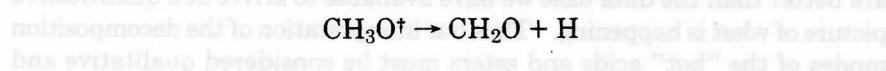
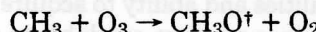
### *Limitations of the Model*

The mechanism used here is predicated on the assumption that the initially formed peroxy radical isomerizes to a "hot" acid or ester, which in turn decomposes to  $CO$ ,  $CO_2$ ,  $H_2O$ , radicals, etc. The formation of a "hot" ester involves an alkyl radical migration, which is known to occur in other biradicals [35-37]. Thus the formation of "hot"  $CH_3COCH_3$  from  $(CH_3)_2COO$  appears to be reasonable. There is some question, however, as to whether alkyl radical migration could compete with hydrogen atom migration in the same molecule. Thus it is not at all clear that  $(CH_3)HCOO$  could isomerize to the "hot" ester  $HCOOCH_3$  in view of the competing reaction leading to the "hot" acid,  $CH_3COOH$ .

Aside from the initiating sequences of reactions, Tables II and III list about 30 secondary free-radical reactions. Other reactions may be involved. In some cases, for example, the reactions involving  $H$ ,  $OH$ ,  $O_2$ ,  $O_3$ ,  $HO_2$ , and  $HCO$ , the kinetics are reasonably well known. Other reactions, particularly those involving radical-radical interactions, may be unimportant. There remains, however, a disturbingly large set of reactions for which the kinetic data base is wholly inadequate. These include the following:

(a) The reactions of  $OH$  radicals with alkenes in the presence of  $O_2$ . There is a good and improving data base on the rate constants for reactions of  $OH$  with alkenes. What is not clear is the nature of the products, which are presumably adducts, and the subsequent reactions of the adducts with  $O_2$ . We have written a sequence of reactions for this important type of reaction based on analogies to the corresponding alkyl radical sequence. We do not, however, hazard a guess as to the nature of the product arising from reactions such as the combination of  $C_3H_6(OH)O_2$  radicals. All such processes have been lumped together in reactions (23), (27), (30), and (31).

(b) Under our experimental conditions in which  $[O_2]/[O_3] \approx 20$ , ozone-radical reactions may compete with  $O_2$ -radical reactions. Thus we expect the  $CH_3-O_3$  reaction to be faster than the  $CH_3-O_2$  reaction. We assume the methyl-radical-ozone reaction to involve the sequence



No allowance has been made for quenching of the hot  $\text{CH}_3\text{O}^\dagger$  species, which could lead to a different type of subsequent chemistry.

The only reported rate constant for the reaction of an alkyl radical with ozone is for the  $\text{CH}_3\text{-O}_3$  reaction [14]. All other alkyl-radical-ozone reactions have been lumped into reaction (18),  $\text{R} + \text{O}_3 \rightarrow \text{RO}^\dagger + \text{O}_2$ , and the subsequent chemistry of  $\text{RO}^\dagger$  excluded.

(c) RO radicals, which might be produced from ozone-radical reactions, are also postulated to be primary reaction products, and can also be formed from alkyl peroxy radical disproportionation reactions. They are lost in radical-radical reactions or through reaction with  $\text{O}_2$ . A key number required for the model calculations is the rate constant for the  $\text{CH}_3\text{O} + \text{O}_2$  reaction, for which there are strongly conflicting values. Wiebe and co-workers [16] report a value of  $k_{13} = 1.6 \times 10^6 \text{ cm}^3/\text{mol}\cdot\text{sec}$ , whereas Mendenhall and co-workers [17] report  $k_{13} = 3.5 \times 10^8 \text{ cm}^3/\text{mol}\cdot\text{sec}$ . There is no basis for a rational choice for this number at this time, although a recent determination by Barker and co-workers [32] supports the higher value. The value used in the model,  $2 \times 10^7 \text{ cm}^3/\text{mol}\cdot\text{sec}$ , was arbitrarily chosen to lie between the reported values.

Other classes of alkoxy-radical reaction have not been included in the modeling calculation because of the lack of information. This includes reactions with ozone, alkenes, and aldehydes. The only rate constant available is an upper limit of  $1 \times 10^9 \text{ cm}^3/\text{mol}\cdot\text{sec}$  [14] for the reaction of  $\text{CH}_3\text{O}$  with  $\text{O}_3$ .

(d) The chemistry of acetyl radicals is another area of great uncertainty. Weaver and coworkers [15] have evidence that the oxidation of  $\text{CH}_3\text{CO}$  radicals leads exclusively to  $\text{CO}_2$ , with no CO being produced. Under our experimental conditions, however, other reaction paths might be important.

(e) The chemistry leading to formation of organic acids is not included in the model. Although the organic acids are shown in Table I to be minor products at time zero, we have considerable doubt as to their being primary products. The shapes of the yield curves for the acids indicate that, for the most part, they are secondary products. Furthermore, a reaction such as (2d) would suggest that at high pressure acids would become important products. Work at atmospheric pressure [26], however, indicates that the organic acids are minor products under those conditions also. Thus the acids may be formed by oxidation of formyl and acetyl radicals and not in a primary ozone-alkene reaction.

This list includes some of the more obvious inadequacies in the data base used in the modeling studies. Others will probably come to light as we attempt to understand these reactions in greater detail. It is clear, however, that our modeling capabilities and ability to acquire phenomenological data are better than the data base we have available to arrive at a quantitative picture of what is happening. Thus our interpretation of the decomposition modes of the "hot" acids and esters must be considered qualitative and

tentative. As kinetic data become available, additional computer modeling studies will lead to a refinement in the model presented here.

### *Mechanisms of Decomposition of Acids and Esters Deduced from Photochemical Studies*

In considering the decomposition of "hot" acids and esters which might be formed in ozone-olefin reactions, we have included reactions which differ greatly in activation energy. For example (as noted by one of the referees) the reaction  $\text{CH}_3\text{COOH} \rightarrow \text{CH}_3 + \text{COOH}$  has an activation energy about 100 kJ lower than the reaction  $\text{CH}_3\text{COOH} \rightarrow \text{CH}_3\text{CO} + \text{OH}$ , and it might be expected that the latter reaction would not be competitive.

Independent studies on the mercury photosensitized decomposition of acids and esters lend support to the mechanism used here. With mercury/photosensitization at 253.7 nm, formic acid can be excited by 471.5 kJ/mol. The calculations of Wadt and Goddard [11] indicate that for the ethylene-ozone reaction the formic acid formed from the isomerization of  $\text{CH}_2\text{O}_2$  will have a minimum of about 400 kJ/mol of excess energy. This suggests that the two systems might be comparable.

Using a mass spectrometric technique to detect free-radical and molecular products, Lossing and co-workers [18,19] have studied the mercury-photosensitized decomposition of acids and esters. The experiments were carried out using a few tenths of a Pa of reactant in 1.06 kPa of helium. The results are given in Table IV. In the case of formic acid, the ratio of CO to  $\text{CO}_2$  is 2.3, which is almost identical to the ratio  $k_{2a}/(k_{2b} + k_{2c}) = 2.5$  (see Table II), strongly supporting the branching ratios deduced in our study of the ozone-ethylene reaction. There was no evidence in the mercury-photosensitization work for reaction (2c) which yields atomic hydrogen. Gorden and Ausloos [20], however, using isotopic labeling and scavenger experiments, were able to show that there is an important free-radical component in both the direct and the mercury-photosensitized photolysis.

The interpretation of the other systems studied is subject to much greater uncertainty. However, the data in general support the choice of decomposition mechanisms used in the present work. The direct photolysis and mercury-photosensitized photolysis of these acids and esters have also been studied by Ausloos and Steacie [21] and by Ausloos [22] whose results in general support the assignments of Table IV.

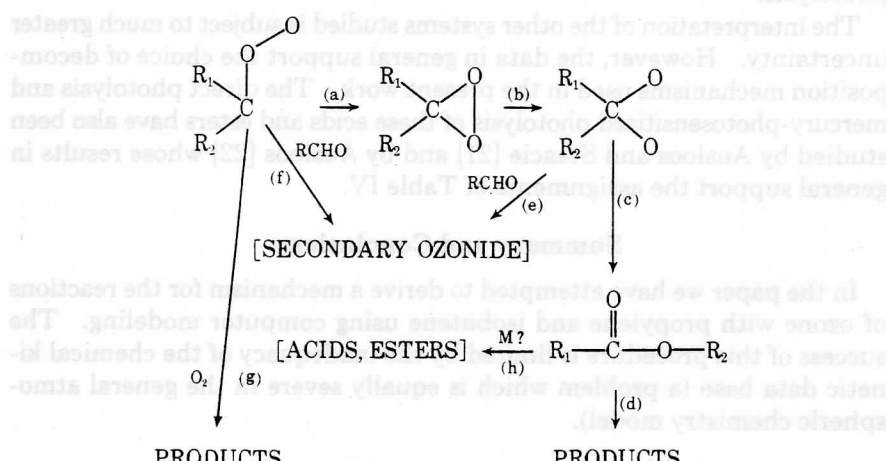
### **Summary and Conclusions**

In the paper we have attempted to derive a mechanism for the reactions of ozone with propylene and isobutene using computer modeling. The success of this procedure is limited by the inadequacy of the chemical kinetic data base (a problem which is equally severe in the general atmospheric chemistry model).

TABLE IV. Low-pressure mercury-photosensitized decomposition of acids and esters at 253.7 nm.

Acid or Ester	Products	Branching Ratio	Reference
HCOOH	H <sub>2</sub> O + CO	0.7	
	H <sub>2</sub> + CO <sub>2</sub>	0.3	
CH <sub>3</sub> COOH	CH <sub>3</sub> CO + OH	> 0.29	18
	CH <sub>3</sub> + H + CO <sub>2</sub>	> 0.18	
	CH <sub>4</sub> + CO <sub>2</sub>	< 0.19	
	CH <sub>2</sub> CO + H <sub>2</sub> O	< 0.24	
HCOOCH <sub>3</sub>	HCO + CH <sub>3</sub> O	0.6	18
	CH <sub>3</sub> + H + CO <sub>2</sub>	0.13	
	CH <sub>3</sub> OH + CO	0.12	
	CH <sub>4</sub> + CO <sub>2</sub>	0.05	
CH <sub>3</sub> COCH <sub>3</sub>	CH <sub>3</sub> CO + CH <sub>3</sub> O	0.8	19
	2CH <sub>3</sub> + CO <sub>2</sub>	0.2	

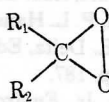
The key problem in ozone-alkene chemistry in the gas phase is the fate of the peroxy radical formed in the initial reaction. There are conflicting theories as to the fate of this species—whether it decomposes to molecular or free-radical products, and/or whether it reacts with O<sub>2</sub>, O<sub>3</sub>, olefins, aldehydes, etc. [23–25].



Isotopic labeling experiments [29] using aldehydes labeled with O<sup>18</sup> appear to rule out reaction (e) as a route to the formation of secondary ozonides in solution, since the O<sup>18</sup> is incorporated almost exclusively in the ether position. Reaction (f), therefore, must be the source of the secondary ozonides observed in studies of ozone olefin reactions in solution and probably in the gas phase at atmospheric pressure [26-28]. In a low-pressure photoionization mass spectrometry study of the reaction of ozone with *cis*-2-butene, a peak in the mass spectrum corresponding to the adduct C<sub>4</sub>H<sub>8</sub>O<sub>3</sub> was observed [2]. Although it was suggested that this was likely to be the hydroperoxide, it could be the secondary ozonide, indicating that reaction (f) occurs also at low pressure.

There is thus some evidence to indicate that the initial steps in the reaction may be the same at low and high pressures. Even the yields of organic acids and esters do not appear to differ greatly at low and high pressures, indicating that reaction (h) may be unimportant or that acids and esters are formed in part in secondary reactions. If the secondary ozonide is formed in low- and high-pressure experiments, it is likely that the initially formed peroxy radical has a finite lifetime, and that reaction (a) is rate limiting with respect to products formed in the reaction sequence (a) to (d).

In summary the mechanism given above involving the sequence (a) to (d) and (f) is in accord with the observation of the intermediate species



the formation of secondary ozonides, and the evidence available from studies of the photolysis of acids and esters. There is no independent evidence to support the postulate of reaction (g) or any other reaction of the various forms of the initially formed carbon peroxide with O<sub>2</sub>, O<sub>3</sub>, alkenes, etc., other than (f).

### Acknowledgment

This work was supported by the Office of Air and Water Measurement, National Bureau of Standards, Washington, DC.

## Bibliography

- [1] J. T. Herron and R. E. Huie, *J. Am. Chem. Soc.*, **99**, 5430 (1977).
- [2] R. Atkinson, B. J. Finlayson, and J. N. Pitts, Jr., *J. Am. Chem. Soc.*, **95**, 7592 (1973).
- [3] B. J. Finlayson, J. N. Pitts, Jr., and R. Atkinson, *J. Am. Chem. Soc.*, **96**, 5356 (1974).
- [4] K. H. Becker, U. Schurath, and H. Seitz, *Int. J. Chem. Kinet.*, **6**, 725 (1974).
- [5] J. T. Herron and R. E. Huie, *J. Phys. Chem.*, **78**, 2085 (1974).
- [6] R. E. Huie and J. T. Herron, *Int. J. Chem. Kinet.*, **S1**, p. 165 (1975).
- [7] F. S. Toby, S. Toby, and H. E. O'Neal, *Int. J. Chem. Kinet.*, **8**, 25 (1976).
- [8] S. M. Japar, C. H. Wu, and H. Niki, *J. Phys. Chem.*, **80**, 2057 (1976).
- [9] R. L. Brown, "A Computer Program for Solving Systems of Chemical Rate Equations," Interim Rep. NBSIR 76-1055, Natl. Bur. Stand., U.S., to appear.
- [10] C. W. Gear, "Numerical Initial Value Problems in Ordinary Differential Equations," Prentice-Hall, Englewood Cliffs, N.J., 1971.
- [11] W. R. Wadt and W. A. Goddard III, *J. Am. Chem. Soc.*, **97**, 3004 (1975).
- [12] F. J. Lovas and R. D. Suenram, *Chem. Phys. Lett.*, **51**, 453 (1977).
- [13] R. I. Martinez, R. E. Huie, and J. T. Herron, *Chem. Phys. Lett.*, **51**, 457 (1977).
- [14] R. Simonaitis and J. Heicklen, *J. Phys. Chem.*, **79**, 298 (1975).
- [15] J. Weaver, J. Meagher, R. Shortridge, and J. Heicklen, *J. Photochem.*, **4**, 341 (1975).
- [16] H. A. Wiebe, A. Villa, T. M. Hellman, and J. Heicklen, *J. Am. Chem. Soc.*, **95**, 7 (1973).
- [17] G. D. Mendenhall, D. M. Golden, and S. W. Benson, *Int. J. Chem. Kinet.*, **7**, 725 (1975).
- [18] P. Kebarle and F. P. Lossing, *Can. J. Chem.*, **37**, 389 (1959).
- [19] R. F. Pottie and F. P. Lossing, *Can. J. Chem.*, **39**, 1900 (1961).
- [20] R. Gorden, Jr. and P. Ausloos, *J. Phys. Chem.*, **65**, 1033 (1961).
- [21] P. Ausloos and E. W. R. Steacie, *Can. J. Chem.*, **33**, 1530 (1955).
- [22] P. Ausloos, *Can. J. Chem.*, **36**, 383 (1958).
- [23] K. L. Demerjian, J. A. Kerr, and J. G. Calvert, *Adv. Environ. Sci. Tech.*, **4**, 1 (1974).
- [24] D. N. McNelis, L. Ripperton, W. E. Wilson, P. L. Hanst, and B. W. Gay, Jr., "Removal of Trace Contaminants from the Air," V. R. Deitz, Ed., ACS Symp. ser. 17, American Chemical Society, Washington, DC, 1975, p. 187.
- [25] T. A. Walter, J. J. Bufalini, and B. W. Gay, Jr., *Environ. Sci. Tech.*, **11**, 382 (1977).
- [26] W. E. Scott, E. R. Stephens, P. L. Hanst, and R. C. Doerr, "Proc. Am. Petroleum Inst.," vol. 37, sec. III—Refining, p. 171 (1957). These results are also included in [27], p. 168.
- [27] P. A. Leighton, "Photochemistry of Air Pollution," Academic Press, New York, 1961.
- [28] H. Niki, P. D. Maker, C. M. Savage, and L. P. Breitenback, *Chem. Phys. Lett.*, **46**, 327 (1977).
- [29] C. W. Gillies, R. P. Lattimer, and R. L. Kuczkowski, *J. Am. Chem. Soc.*, **96**, 1536 (1974).
- [30] R. F. Hampson, Jr., and D. Garvin, Eds., "Chemical Kinetic and Photochemical Data for Modeling Atmospheric Chemistry," Tech. Note 866, Natl. Bur. Stand., U.S., June 1975. U.S. Government Printing Office, Washington, DC 20402.
- [31] M. J. Kurylo, N. C. Peterson, and W. Braun, *J. Chem. Phys.*, **53**, 2776 (1970).
- [32] J. R. Barker, S. W. Benson, and D. M. Golden, *Int. J. Chem. Kinet.*, **9**, 31 (1977).
- [33] N. Washida and K. D. Bayes, *Int. J. Chem. Kinet.*, **8**, 777 (1976).
- [34] W. Braun and M. Lenzi, *Disc. Faraday Soc.*, **44**, 252 (1967).
- [35] R. J. Cvitanovic, *Can. J. Chem.*, **36**, 623 (1958).
- [36] R. Klein and M. D. Scheer, *J. Phys. Chem.*, **74**, 613 (1970).
- [37] M. C. Flowers, R. M. Parker, and M. A. Voisey, *J. Chem. Soc. B*, 239 (1970).

- [38] R. Atkinson and J. N. Pitts, Jr., *J. Chem. Phys.*, **63**, 3591 (1975).
- [39] C. H. Wu, S. M. Japar, and H. Niki, *J. Environ. Sci. Health*, **A11**, 191 (1976).

Received September 1, 1977

Revised January 10, 1978